

FIBRE-OPTIC SENSORS

PACS numbers: 42.81.Gs; 42.81.Pa
DOI: 10.1070/QE2014v044n10ABEH015387

Modified sensing element of a fibre-optic current sensor based on a low-eigenellipticity spun fibre

Ya.V. Przhiyalkovsky, S.K. Morshnev, N.I. Starostin, V.P. Gubin

Abstract. **We have proposed and investigated a modified sensing element of a spun fibre current sensor for the case when the beat length of the built-in linear birefringence of the fibre is equal to or less than the spin pitch of its helical structure. The proposed configuration makes it possible to restore the interferometer contrast reduced because of the decrease in the ellipticity of the wavelength-averaged polarisation state of radiation propagating in such spun fibre. The modified sensing element contains two polarisation state converters: one, located at the spun fibre input, produces polarisation with ellipticity equal to the eigenellipticity of the fibre, and the other ensures conversion of the elliptical polarisation to an orthogonal one through mirror reflection at the fibre output. We have also demonstrated that the magneto-optical sensitivity decreases slightly for the analysed spectrum-averaged parameters of the polarisation state of radiation in the spun fibre. Experimental data lend support to the theoretical predictions.**

Keywords: *current sensor, Faraday effect, spun fibre.*

1. Introduction

Spun optical fibre with a helical structure of its linear birefringence (BR) axes is at present widely used as a sensing element in Faraday effect fibre-optic current sensors (FOCS's). The operating principle of the FOCS's is to measure, using interferometry, the phase difference between two light waves that have orthogonal circular polarisation states (PS's) and propagate through a spun fibre. In the case of the Faraday effect, the phase difference is proportional to the longitudinal component (parallel to the wave propagation direction) of the magnetic field generated by the current to be measured.

One possible FOCS configuration, which has already become traditional, is a low-coherence reciprocal linear reflective interferometer [1]. In such interferometers, two orthogonal circularly polarised light waves are generated using a $\lambda/4$ plate. After passing through a magnetic field-sensitive spun fibre, the light waves are mirror-reflected from its end and travel in the reverse direction. The mirror reflection changes the circular PS's of the waves to orthogonal. In this way, all reciprocal effects during the propagation through the optical path are compensated for, and the optical path difference between the signal waves of the interferometer is only determined by the nonreciprocal Faraday effect.

To obtain high (~100%) contrast, the conventional interferometer configuration requires spun fibres with low values (below 0.3) of the parameter $\sigma = L_{tw}/(2L_b)$, where L_{tw} is the spin pitch in the helical fibre structure and L_b is the beat length of the built-in linear BR of the fibre [2]. When this condition is fulfilled, the spun fibre is capable of supporting a so-called quasi-circular PS of light, i.e. a PS whose spectrum-averaged ellipticity approaches that of a circular PS. Given that the minimum spin pitch in classical spun fibre drawing technology is $L_{tw} \approx 2.5–3$ mm, the minimum value of L_b is ~7–8 mm.

On the other hand, the stability of spun fibres to external influences, in particular to bending, is determined by their built-in linear BR [3, 4]. For this reason, the sensing elements of FOCS's with a small loop radius (~1 cm or less) should employ spun fibres with higher BR ($L_b \approx 2–3$ mm). In practice, this means the use of spun fibres with high σ (over 0.3). This issue is of considerable current interest because there is a broad class of magnetosensitive spun microstructured fibres with a beat length from 0.1 to 3 mm [3, 5, 6] that offer excellent temperature stability of their BR and effectively build up the Faraday phase shift even at a loop radius of ~2 mm [3], which makes them extremely attractive for application in FOCS's. At the same time, the intrinsic polarisation ellipticity of high-σ spun microstructured fibres (i.e. their ability to maintain a PS with a particular mean ellipticity of optical radiation) differs markedly from a circular PS [2]. If they will be used in a conventional FOCS configuration, the interference fringe contrast will be considerably reduced because of the presence of incoherent light components in the interferometer [6] due to the irreversible depolarisation of broadband radiation in the sensing element.

In this report, we propose a modified sensing element for a current sensor which allows one to avoid the development of a considerable incoherent component of broadband radiation in an interferometer and, as a consequence, to minimise the associated contrast loss. The new configuration is implemented and investigated theoretically and experimentally.

Ya.V. Przhiyalkovsky, S.K. Morshnev, N.I. Starostin, V.P. Gubin
V.A. Kotel'nikov Institute of Radio Engineering and Electronics (Fryazino Branch), Russian Academy of Sciences, pl. Vvedenskogo 1, 141190 Fryazino, Moscow region, Russia; Profotech CJSC, Vereiskaya ul. 17, 121357 Moscow, Russia;
e-mail: yankus.p@gmail.com, nis229@ire216.msk.su

Received 17 January 2014; revision received 3 March 2014
Kvantovaya Elektronika **44** (10) 957–964 (2014)
Translated by O.M. Tsarev

2. Use of high-σ spun fibres in the sensing element of FOCS's

Consider first an FOCS built upon an interferometer principle, with an ideal isotropic fibre as a conventional magnetosensitive element (Fig. 1). The broadband optical radiation from a source (*1*) passes through a directional coupler (*2*) and fibre polariser (*3*), which converts it to linearly polarised radiation. Next, the radiation is coupled into a linear polarisation-maintaining (PM) fibre (*4*). The BR axes of the PM fibre are oriented at an angle of 45° to the transmission axis of the polariser. As a result, two waves identical in intensity, with linear orthogonal PS's propagate through the fibre. While propagating through the PM fibre, the waves become incoherent. When passing through a quarter-wave plate (*5*), the waves acquire circular polarisation. Next, they enter a magnetosensitive fibre (*6*), which forms a closed loop around a current-carrying conductor. At the output of the fibre (*6*), the waves are reflected from a mirror (*7*), which changes their polarisation to orthogonal, and pass the same path in the reverse direction, restoring coherence. The two waves interfere at the polariser (*3*) and arrive at a photodetector (*8*) through the directional coupler (*2*).

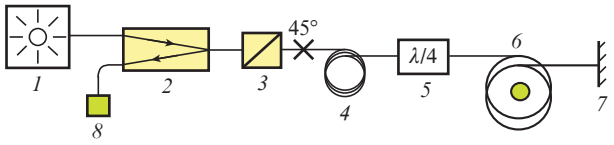

Figure 1. Reciprocal reflective interferometer configuration (see text for notation).

In this configuration, after the linearly polarised light is split into two orthogonally polarised waves, the PS's of both waves are converted by the components of the scheme so that they always remain orthogonal. Consider the evolution of one of the waves on the Poincare sphere (Fig. 2). The $\lambda/4$ plate changes the linear PS at point A to the left-hand circular PS represented by point L (Fig. 2a). When light propagates through an ideal isotropic fibre, its PS remains unchanged, but mirror reflection converts it to a right-hand circular PS (Fig. 2b, point R), which persists when the light propagates in the reverse direction. The $\lambda/4$ plate converts the PS of the wave to a linear PS (point B) orthogonal to the original one (point A) (Fig. 2c). It can be shown in a similar way that, as the other wave propagates in the forward and reverse directions, its linear PS experiences the same changes as in the case of the former wave. As a result, in the absence of any current across the loop (*6*) (Fig. 1) the two waves pass the same optical path and restore coherence with each other at the polariser, which ensures a near 100% interferometer contrast.

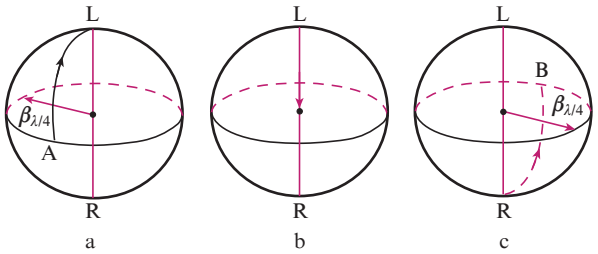

Figure 2. Evolution of the PS of one of the orthogonally polarised waves in a conventional configuration of the sensing element of a reciprocal reflective interferometer. $\beta_{\lambda/4}$ is the BR vector of the quarter-wave plate.

As mentioned above, under strong internal influences or at small dimensions of sensing fibre loops it is reasonable to use a spun highly birefringent (HiBi) fibre ($\sigma > 0.3$). The spectrum-averaged PS of waves propagating through such fibre is elliptical [2]. This leads to the irreversible depolarisation of broadband radiation, produces an incoherent component in an interferometer with a conventional sensing element and, hence, diminishes the contrast, which in turn reduces the detectivity of the current sensor. The optical circuit of such an interferometer has several points where radiation is partially depolarised. First, the degree of polarisation decreases when light propagates in the forward direction and enters the spun fibre, as a result of the conversion of the (initial) circular PS to a PS with ellipticity equal to the eigenellipticity [2]. Second, the degree of polarisation decreases because mirror reflection converts an elliptical PS to another elliptical PS, nonorthogonal to the initial one [6]. Third, partial depolarisation occurs when the light passes through the $\lambda/4$ plate in the reverse direction, because an elliptical PS (with eigenellipticity) is converted by the plate to another elliptical (nonlinear) PS.

To prevent light depolarisation in the interferometer and avoid contrast reduction when spun fibre with a high σ of the sensing element is used, we propose a modified sensing element configuration (Fig. 3). It follows from analysis of PS evolution in spun fibre [2] that, when the fibre is excited by broadband radiation whose PS has ellipticity equal to the eigenellipticity of the fibre and an azimuth coinciding with that of one of its built-in linear BR axes, the radiation propagates through the fibre with no reduction in its degree of polarisation. Thus, replacing the $\lambda/4$ plate in the sensing element of the FOCS by an elliptical phase plate (*9*) converting the initial, linear PS to an elliptical PS with eigenellipticity, and orienting the built-in BR axes of the spun fibre so that they make an angle of 45° with the axes of the elliptical plate, one can avoid the first reduction in the degree of polarisation, when light propagates through the optical circuit in the forward direction [from the phase plate (*9*) to the magnetosensitive spun fibre (*6*)].

Consider now light reflection from the end of the sensing element of an FOCS. Only a circular PS is converted by a mirror to an orthogonal PS. To convert elliptically polarised light incident on a mirror to light with an orthogonal PS, another phase plate (*10*), converting the elliptical PS at the spun fibre output to a circular PS, should be placed in front of the mir-

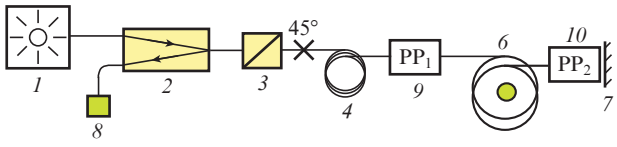

Figure 3. Configuration of an FOCS with a modified sensing element (see text for notation).

ror (*7*). When light waves are reflected from the mirror and pass through plate *10* in the reverse direction, their PS converts to that orthogonal to the initial elliptical PS. Because of this, when the light waves propagate through the spun fibre in the reverse direction, the degree of polarisation of the light remains unchanged. During further light propagation in the reverse direction, plate *9* changes the PS of the light to a linear PS orthogonal to its initial PS at the input of plate *9* in the forward direction. Therefore, after a round trip through the optical circuit, the degree of polarisation of the light remains close to 100% and the incoherent component is minimal.

Thus, in the proposed modified sensing element, the PS's of the two waves are converted by optical components so that they always remain orthogonal. As an example, consider the evolution of the PS of one of the waves on the Poincare sphere (Fig. 4). The first elliptical phase plate, whose axes make an angle of 45° with the BR axes of the input PM fibre, changes the initial, linear PS (point A) to a PS with ellipticity equal to the eigenellipticity of the spun fibre and an azimuth equal to the initial azimuth of its BR axis (Fig. 4a, point U). When a wave propagates in a spun fibre, only the azimuth of its PS varies, whereas its ellipticity remains unchanged [2], which corresponds to movement along a constant-latitude circle on the Poincare sphere (Fig. 4b). Under such excitation conditions, the degree of polarisation remains 100%. The second phase plate, located at the end of the spun fibre and oriented with its axes at 45° to the BR axes of the spun fibre, brings the PS to a circular one (Fig. 4c, point L). It is worth noting here that, on the whole, the two plates change a linear PS to a circular one, i.e., provided they are made from the same birefringent material, the sum of their lengths is equal to the length of a $\lambda/4$ plate from the same material and the ratio of the lengths of the first and second phase plates is equal to the ratio of the latitude for the eigenellipticity of the spun fibre to its colatitude.

Next, the light is reflected from the mirror (Fig. 4d), which changes its PS from left-hand circular (point L) to orthogonal right-hand circular (point R). After the light passes through the second phase plate in the reverse direction, its PS is automatically converted from right-hand circular (point R) to elliptical (point V), orthogonal to the state at point U, with eigenellipticity and an azimuth equal to that of the BR of the spun fibre (Fig. 4e). When the light passes through the spun fibre in the reverse direction, the azimuth of its PS rotates in the opposite sense relative to forward propagation (Fig. 4f). During further propagation of the light, its PS is converted by the first plate (*9*) to a linear PS (point B), orthogonal to the initial one (Fig. 4g, point A).

3. Theory of the modified spun-fibre sensing element

Consider first in greater detail the modified sensing element of a FOCS in the case of monochromatic radiation. Analysis will be carried out in the Jones matrix approach. As a laboratory coordinate system of PS's, we take a system of circular polarisations. Let the BR vector of the input PM fibre in the sensing element point to a horizontal linear PS on the Poincare sphere, which corresponds to such a spatial Cartesian coordinate system in which the x and y axes are collinear with the birefringence axes of the PM fibre and the z axis is directed along the fibre axis in the propagation direction of the light.

In subsequent description, we use the auxiliary matrices

$$T_1 = \begin{pmatrix} \exp(\mathrm{i}\alpha/2) & 0 \\ 0 & \exp(-\mathrm{i}\alpha/2) \end{pmatrix}, \qquad T_2 = \begin{pmatrix} \cos(\varphi/2) & \sin(\varphi/2) \\ -\sin(\varphi/2) & \cos(\varphi/2) \end{pmatrix}. \tag{1}$$

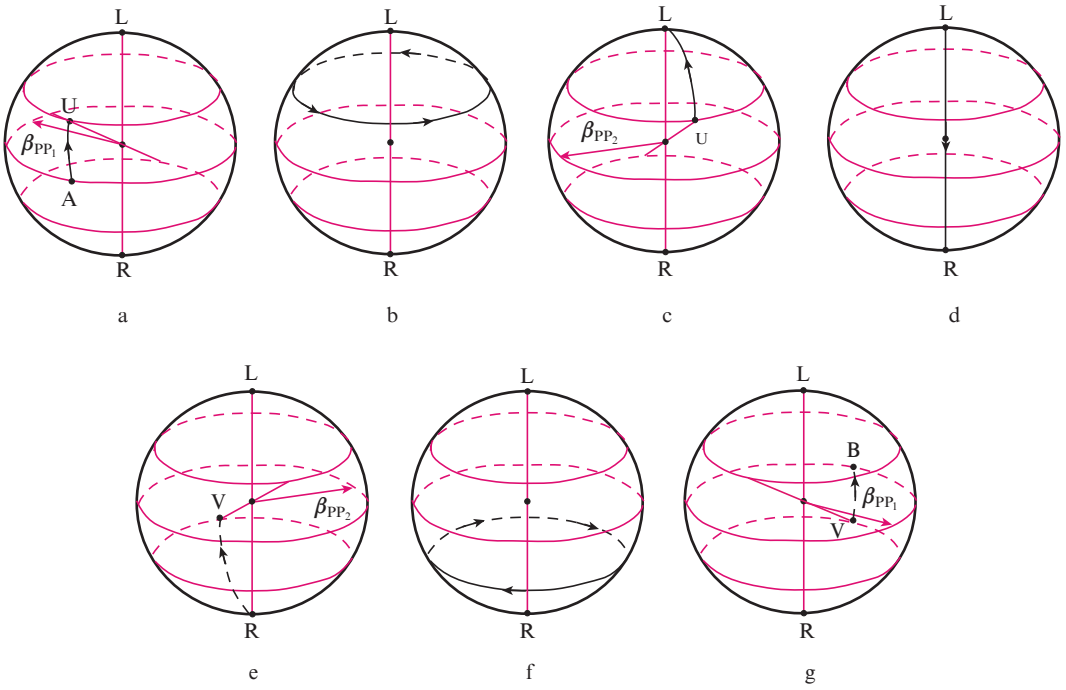

Figure 4. Evolution of the PS of one of the orthogonally polarised waves in a modified configuration of the sensing element of a reciprocal reflective interferometer. β_{PP_1} and β_{PP_2} are the BR vectors of the first and second phase plates.

These matrices can be regarded as the matrices of PS coordinate system transformations, namely, those of rotations of the Poincare sphere. Matrix T_1 represents a rotation of the sphere about axis RL through angle α, and matrix T_2 represents a rotation of the sphere about axis PQ through angle φ (Fig. 5). At the same time, these matrices can be used as Jones matrices of optical components that perform inverse transformations of the PS of light waves: the effect of the component represented by matrix T_1 is equivalent to a rotation of the point representing the PS on the (immobile) sphere about axis RL through angle $-\alpha$, and that of the component represented by matrix T_2 is equivalent to a rotation of the PS on the sphere about axis PQ through angle $-\varphi$. Note in this context that the inverse matrices of T_i for $i = 1, 2$ are equivalent to rotations through a negative angle, $T_i^{-1}(\alpha) = T_i(-\alpha)$, and that the product of two matrices, $T_i(\alpha)T_i(\beta)$, is equal to the matrix representing a rotation through the sum angle, $T_i(\alpha + \beta)$.

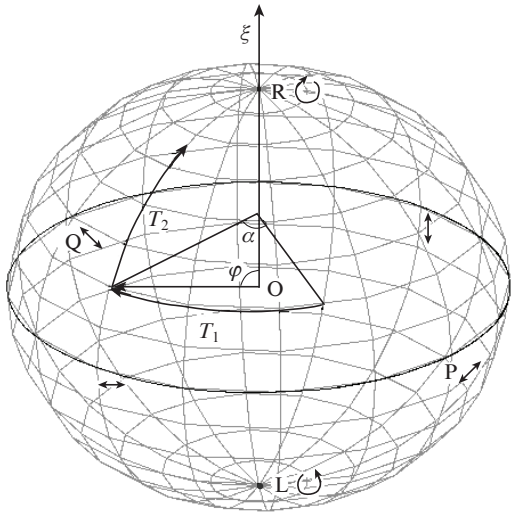

Figure 5. Rotations of the Poincare sphere represented by matrices T_1 and T_2 for transformations of the coordinate system of polarisation states.

We will use these matrices for describing phase plates and diagonalising the differential Jones matrix of the spun fibre, as was done previously [2], similarly to the diagonalisation of equations of coupled modes for an anisotropic medium with a helical structure of its linear BR [7, 8].

The first phase plate of the modified sensing element of the FOCS is located between PM fibre and magnetosensitive spun fibre, and the angle between the BR axes at the end of the PM fibre and the BR axes of the plate is 45°. The phase difference introduced by the phase plate is determined by the linear BR beat length of the plate material, L_{b0}, and the thickness of the plate, L. In particular, the plate can be made from a PM fibre segment. Let the BR vector of the plate be directed towards a linear PS on the Poincare sphere with a latitude of $-\pi/2$ (Fig. 5, point Q). In the laboratory system of circular polarisations, the Jones matrix of such a phase plate has the form

$$M_1^+ = T_2(-\varphi), \tag{2}$$

where $\varphi = 2\pi L/L_{b0}$ is the phase angle introduced by the fibre plate between the linear x and y polarisation modes of the light.

The first phase plate should produce a PS whose ellipticity is equal to the eigenellipticity of the spun fibre (Fig. 4a). The eigenellipticity of the spun fibre is determined by its σ [2] and can be found as

$$e = \sqrt{\sigma^2 + 1} - \sigma. \tag{3}$$

Therefore, to obtain an eigenellipticity PS using a phase plate, the minimum length of the plate should meet the relation

$$\varphi = 2\pi\frac{L}{L_{b0}} = 2\arctan e = \frac{\pi}{2} - \arctan\sigma. \tag{4}$$

The length of the first phase plate is then

$$L_1 = L_{\lambda/4}\left(1 - \frac{2}{\pi}\arctan\sigma\right), \tag{5}$$

where $L_{\lambda/4} = L_{b0}/4$ is the length of the quarter-wave plate.

In the case of light travelling in the reverse direction (Fig. 4g), the Jones matrix of the first phase plate has the form

$$M_1^- = T_2(\varphi). \tag{6}$$

Let us calculate the Jones matrix of the spun fibre in the sensing element of the FOCS. As shown earlier [2], in an elliptical coordinate system rotating together with the BR vector the equation for the transformation of the Jones vector of a light wave passing through a spun fibre segment of length L is given by

$$\boldsymbol{E}_e(L) = M_e^+\boldsymbol{E}_e(0). \tag{7}$$

Here, the Jones matrix of the spun fibre segment has a diagonal form,

$$M_e^+ = \begin{pmatrix} \exp[\frac{1}{2}i\Omega(\gamma)L] & 0 \\ 0 & \exp[-\frac{1}{2}i\Omega(\gamma)L] \end{pmatrix} = T_1(\Omega(\gamma)L), \tag{8}$$

and is determined by the parameters of the spun fibre and the circular BR induced by the magnetic field of the electric current through the spatial frequency

$$\Omega(\gamma) = (2\xi + \gamma)\sqrt{1 + \left(\frac{\Delta\beta}{2\xi + \gamma}\right)^2}, \tag{9}$$

where $\gamma = VB_z$ is the rate of the increase in the phase difference between waves with orthogonal circular polarisations because of the Faraday effect-induced circular BR [4]; V is the Verdet constant; B_z is the longitudinal magnetic field component; $\Delta\beta = k_y - k_x = 2\pi/L_b$ is the rate of the increase in the phase difference between waves with orthogonal linear polarisations, determined by the built-in linear BR with a beat length L_b; and $\xi = 2\pi/L_{tw}$ is the spatial rotation frequency of the axes of built-in linear BR with a spin pitch L_{tw}.

In the rotating system of elliptical PS's, the Jones vectors at the input and output ends of the spun fibre can be expressed through the Jones vectors in the system of circular PS's and transition matrices as follows:

$$\boldsymbol{E}_{\mathrm{e}}(0) = T_2(0)T_1(0)\boldsymbol{E}_{\mathrm{c}}(0),$$
$$\boldsymbol{E}_{\mathrm{e}}(L) = T_2(\varphi)T_1(-\alpha_{\mathrm{L}})\boldsymbol{E}_{\mathrm{c}}(L), \tag{10}$$

where α_{L} is the angle through which the built-in linear BR vector of the spun fibre rotates towards its output end. Substituting these expressions into Eqn (7), we find the Jones matrix of the spun fibre segment for light propagating in the forward direction in the coordinate system of circular PS's:

$$M_{\mathrm{c}}^{+} = T_1^{-1}(-\alpha_{\mathrm{L}})T_2^{-1}(\varphi)M_{\mathrm{e}}^{+}T_2(\varphi). \tag{11}$$

Reflection from the mirror reverses the propagation direction of the light relative to the longitudinal component of the magnetic field vector, so in the rotating elliptical coordinate system the Jones matrix for propagation in the reverse direction has the form

$$M_{\mathrm{e}}^{-} = \begin{pmatrix} \exp[-\frac{1}{2}\mathrm{i}\Omega(-\gamma)L] & 0 \\ 0 & \exp[\frac{1}{2}\mathrm{i}\Omega(-\gamma)L] \end{pmatrix} = T_1(-\Omega(-\gamma)L). \tag{12}$$

Similarly, multiplying M_{e}^{-} by rotation matrices we find the Jones matrix of the spun fibre for the reverse direction in the coordinate system of circular PS's:

$$M_{\mathrm{c}}^{-} = T_2^{-1}(\varphi)M_{\mathrm{e}}^{-}T_2(\varphi)T_2(\alpha_{\mathrm{L}}). \tag{13}$$

The second phase plate, located after the spun fibre segment of length L_1, brings the ellipticity of the PS to circular, i.e. changes the latitude on the Poincare sphere from φ to $\pi/2$. Therefore, the thickness of this plate is $L_2 = L_{\lambda/4} - L_1$. With allowance for the rotation of the BR axes of the spun fibre through angle α_{L} at the output end of the segment, the Jones matrices of the second plate for light propagation in the forward and reverse directions have the form

$$M_2^{+} = T_1(\alpha_{\mathrm{L}})\,T_2\Big(-\Big(\frac{\pi}{2} - \varphi\Big)\Big)\,T_1(-\alpha_{\mathrm{L}}),$$
$$M_2^{-} = T_1(-\alpha_{\mathrm{L}})\,T_2\Big(\frac{\pi}{2} - \varphi\Big)\,T_1(\alpha_{\mathrm{L}}). \tag{14}$$

Behind the second phase plate, there is a mirror, whose Jones matrix transforms the coordinate system according to the reversal of the propagation direction of the light. The circular PS of each wave then changes to an orthogonal PS with a phase shift by π:

$$Z = \begin{pmatrix} 0 & -1 \\ -1 & 0 \end{pmatrix}. \tag{15}$$

To obtain the overall Jones matrix of the entire sensing element of the FOCS, the Jones matrices should be multiplied in the order of light propagation from right to left and, for adequate comparison (in the same coordinate system), the product should be premultiplied by the matrix of the mirror, Z:

$$M = ZM_1^{-}M_{\mathrm{c}}^{-}M_2^{-}ZM_2^{+}M_{\mathrm{c}}^{+}M_1^{+} \tag{16}$$
$$= \begin{pmatrix} 0 & -\exp\{-\frac{1}{2}\mathrm{i}[\Omega(\gamma) - \Omega(-\gamma)]L\} \\ \exp\{\frac{1}{2}\mathrm{i}[\Omega(\gamma) - \Omega(-\gamma)]L\} & 0 \end{pmatrix}.$$

Consider in greater detail the spatial frequency difference in the exponents in (16). Note that the Faraday effect in silica fibre is rather weak and the beat length of the associated circular BR is in practice much greater than the beat length of the built-in linear BR and the spin pitch of the helical structure, which usually are several millimetres. In other words, the inequalities $\gamma \ll \xi$ and $\gamma \ll \Delta\beta$ are satisfied with high accuracy. Expanding $\Omega(\gamma)$ into a power series in γ and retaining only the first-order terms, we obtain

$$\Omega(\gamma) \approx 2\xi\sqrt{1+\sigma^2} + \frac{\gamma}{\sqrt{1+\sigma^2}} = \Omega_0 + S\gamma, \tag{17}$$

where Ω_0 is the spatial frequency $\Omega(0)$ in the absence of circular BR and $S = 1/\sqrt{1+\sigma^2}$. Therefore,

$$\Omega(\gamma) - \Omega(-\gamma) = 2\mathrm{S}\gamma. \tag{18}$$

It is seen from (17) that the phase difference ΩL that the light waves acquire when propagating in the forward direction comprises two terms: $\Omega_0 L$ and $S\gamma L$. The former term is only determined by the built-in parameters of the fibre, and the latter is determined by the magnetic field. Relation (18) means that, when light propagates in the reverse direction, the γ-independent term $\Omega_0 L$ in the phase difference is fully compensated and the resultant phase difference is only determined by the magnetic field.

Thus, the final matrix of the optical system is

$$M = \begin{pmatrix} 0 & -\exp(-\mathrm{i}S\gamma L) \\ \exp(\mathrm{i}S\gamma L) & 0 \end{pmatrix}. \tag{19}$$

If input radiation in the optical system has a linear PS oriented at 45° to the horizontal axis, which corresponds to excitation of two, x- and y-polarised waves in the PM fibre (*4*) (Fig. 1), at the output of the system it converts to

$$\boldsymbol{E}_{\mathrm{c}}^{\mathrm{out}} = \begin{pmatrix} 0 & -\exp(-\mathrm{i}S\gamma L) \\ \exp(\mathrm{i}S\gamma L) & 0 \end{pmatrix}\frac{1}{2}\begin{pmatrix} 1-\mathrm{i} \\ 1+\mathrm{i} \end{pmatrix} = -\frac{\mathrm{i}}{2}\begin{pmatrix} (1-\mathrm{i})\exp(\mathrm{i}S\gamma L) \\ (1+\mathrm{i})\exp(-\mathrm{i}S\gamma L) \end{pmatrix}. \tag{20}$$

In the coordinate system of linear polarisations, vector (20) is expressed as

$$\boldsymbol{E}_{\mathrm{lin}}^{\mathrm{out}} = -\mathrm{i}\begin{pmatrix} \exp(\mathrm{i}S\gamma L) \\ \exp(-\mathrm{i}S\gamma L) \end{pmatrix}. \tag{21}$$

Thus, in the presence of a magnetic field, the modified sensing element introduces a phase difference $\Delta\varphi_m = 2S\gamma L$ between linearly x- and y-polarised waves.

It is worth pointing out that a conventional sensing element that uses an ideal isotropic fibre is the limiting case of the modified sensing element for $\sigma \to 0$: the length of the first phase plate becomes equal to that of the quarter-wave plate and the length of the second plate becomes zero. The phase difference introduced by such a sensing element is then $\Delta\varphi_{id} = 2\gamma L$. Therefore, the coefficient S determines the magnetic sensitivity of the fibre and depends only on the built-in parameters of the fibre.

In the case of an ideal isotropic fibre, the condition $\Delta\beta = 2\pi/L_b \to 0$ is fulfilled, so the coefficient S reaches its maximum value: unity. With increasing built-in linear BR at a constant spin pitch of the helical structure, the eigenellipticity of radiation in the spun fibre shifts from circular towards linear and, hence, the sensitivity to the magnetic field-induced circular BR decreases.

The above analysis for monochromatic light can readily be generalised to the case of broadband radiation provided its bandwidth is small compared to its centre wavelength: $\Delta\lambda \ll \lambda_0$. It should be taken into account that the BR beat length in the phase plates and spun fibre and the circular BR are functions of wavelength. It is, however, easy to show that, to a first approximation, the analysis results for each wavelength in the spectrum are wavelength-independent and are the same for each spectral component. First, since the length of the elliptical plates is small (a fraction of a quarter of the beat length L_{b0}), the distinctions between how the plates change the PS of the spectral components of light are rather small, and the Jones matrices of the plates (2), (6) and (14) can be thought of as wavelength-independent. To a first approximation, one can also neglect the wavelength dependence upon the transition to a rotating coordinate system in (11) and (13) [2]. Second, to a first approximation, one can neglect the wavelength dependence of the product of the Jones matrices of the components of the optical system (19). Consider now the phase difference $2S\gamma L$ that light waves acquire (in the presence of a magnetic field) while passing through the entire optical system. The $V(\lambda)$ dependence [9], which determines the circular BR when $\Delta\lambda \ll \lambda_0$, can be neglected. The coefficient $S = 1/\sqrt{1+\sigma^2}$ is, strictly speaking, also wavelength-dependent, because the parameter σ, which includes the beat length, is wavelength-dependent. It can be shown, however, from the $S(\sigma)$ behaviour that, at a small bandwidth, S is a weak function of wavelength, so the coefficient at the centre wavelength λ_0 can be taken as the average sensitivity coefficient.

It is worth pointing out that the ease of generalisation to the case of broadband radiation is a direct consequence of the ability of the proposed optical configuration to identically convert the PS's of the spectral components of radiation, leaving a point set of the components on the Poincare sphere. At the same time, in the case of a conventional sensing element, the PS's of the spectral components of light will be converted in different ways, which adds much complexity to analysis of such a system and, hence, to generalization to the case of broadband radiation.

Note also that the formula for the magneto-optical sensitivity of spun fibre, $S = 1/\sqrt{1+\sigma^2}$, rigorously derived above, in particular with allowance for broadband radiation, coincides with the sensitivity estimate for monochromatic radiation [6].

4. Experimental

To experimentally verify the above theoretical analysis results, we used elliptical stress cladding spun fibre with $L_{tw} \approx L_b$. To accurately fabricate phase plates, we first measured parameters of the fibre. The spin pitch of the helical structure was measured as described previously [2] and was determined to be $L_{tw} = 26 \pm 1$ mm. The phase BR beat length, also measured as described previously [2], was determined to be $L_b = 21 \pm 0.5$ mm. Built-in linear BR beat length measurements by a widely used spectral method are in this case inadequate because we need to know the phase BR beat length, whereas as shown earlier [10] the spectral method provides the geometric mean of the phase and group BR. The σ of the spun fibre used was calculated to be 0.62 ± 0.04. Note that, since the analysed properties of spun fibres depend on $\sigma = L_{tw}/(2L_b)$, for a given sample in the experiments described below they will be similar to the properties of spun fibre with the same value of σ but a different length L_b, e.g. 2.4 mm, at a typical L_{tw} of 3 mm.

4.1. Contrast measurement for an interferometer with a modified sensing element

To fabricate phase plates, we used an elliptical-core PM fibre with a beat length $L_{b0} = 6.7$ mm. To fabricate the first plate and incorporate it into the optical system, the fibre was fusion spliced in an oriented manner to a segment of an input PM fibre of the PANDA type so that the BR axes of the two fibres made an angle of $45° \pm 1°$. To this end, linearly polarised broadband radiation with the oscillation direction of its electric vector parallel to one of the BR axes of the fibre was coupled into the PM fibre. The elliptical-core PM fibre was fusion spliced to the output end of the PANDA fibre using an oriented fibre splicing apparatus (Fujikura FSM-100PM). The fibres were angle-oriented manually. The criterion for accurate angle orientation of the fibre axes at 45° was the maximum depolarisation of the light at the output of the elliptical-core fibre. The degree of polarisation was analysed using a device described elsewhere [11]. When the maximum depolarisation was reached, the fibres were fusion spliced.

Next, using a fibre cleaver mounted under a microscope, the length of the elliptical-core fibre was reduced so that the distance from the fusion splice to the cleave was equal to the length calculated by (5), $L_1 = 1.11$ mm, with an accuracy of ± 0.02 mm. The phase plate thus produced was fusion spliced to the spun fibre, with the angle between the BR axes corresponding to the maximum degree of polarisation at the other fibre end, as described previously [2].

To fabricate the second phase plate, the end of the spun fibre was fusion spliced to another segment of the same elliptical-core PM fibre, and the degree of polarisation of light was analysed at its output. The fibres were first angle-oriented manually. As in the fabrication of the first plate, the criterion for proper orientation (45° between the BR axes of the fibres) was the maximum depolarisation of the light at the output. Next, the length of the elliptical-core fibre was reduced so that the distance from the fusion splice to the cleave was equal to the

calculated length $L_2 = L_{\lambda/4} - L_1 = 0.56$ mm with an accuracy of ±0.02 mm. Note that the cleave of the second fibre plate served as well as a Fresnel reflector. Next, the input PM fibre of the sensing element was fusion spliced in an oriented manner to the output PM fibre (*4*) of the FOCS (Fig. 3) so that the BR axes of the two fibres were parallel to each other.

We fabricated two sensing elements based on the spun fibre under consideration: one in the conventional configuration, with a $\lambda/4$ plate, and the other in the modified configuration, with two phase plates. The two sensing elements were incorporated one-by-one into the optical scheme of a FOCS [4] and the interference fringe contrast was measured. The contrast was determined to be 43.3% in the configuration with the conventional sensing element and 89.4% for the FOCS with the modified sensing element. That we failed to obtain 100% contrast can be accounted for by the influence of imperfections of the optical components in the sensing element under investigation.

It is worth pointing out that, estimating the interferometer contrast by the relation $K = [1/(1 + \sigma^2)]^2$, which was derived in Ref. [3] for monochromatic radiation and takes into account the incomplete conversion of elliptically polarised waves upon reflection from a mirror, we obtained $K = 52.2\%$, which slightly exceeds the measured contrast of the conventional configuration. The discrepancy can be accounted for by an additional wave coherence loss as a result of the conversion of the wavelength-averaged circular PS to an elliptical PS when the light is coupled into the spun fibre and as a result of the conversion of the elliptical PS by the $\lambda/4$ plate when the light propagates across the plate in the reverse direction.

4.2. Fibre sensitivity measurement

The sensitivity of spun fibre with $\sigma = 0.62$ was measured using a laboratory FOCS [4], which sequentially measured a standard (constant) current with various sensing elements. We used two sensing element configurations having the same number of fibre turns. One had the above modified scheme, with the use of the spun fibre under investigation, and the other used a sensing element based on a reference spun fibre drawn from the same preform but with a spin pitch of the helical structure $L_{tw} = 3$ mm. In this case, the BR beat length was several times the spin pitch of the helical structure ($\sigma \approx 0.07$), so the sensing element with such spun fibre was produced in the conventional configuration with a $\lambda/4$ plate. The interference fringe contrast in the FOCS with the reference spun fibre was 90.7%, which is close to the contrast in the FOCS with the modified sensing element (89.4%), so the possible influence of contrast on standard current measurement can be ruled out. Since the two fibres were drawn from the same preform, their Verdet constants can be thought to be identical to within high accuracy. Under such conditions, during measurements of a standard (constant) current the ratio of the FOCS signals obtained using the sensing elements based on the spun fibres under investigation will be equal to the ratio of the fibre sensitivities.

Measuring the standard current, we obtained 1.865 A in the scheme with the spun fibre under investigation and 2.223 A in the scheme with the reference fibre, i.e. the ratio of the currents is 0.84. Using the relation $S = 1/\sqrt{1 + \sigma^2}$, we find that the ratio of the sensitivities of fibres with these parameters is 0.85. Therefore, the experimental data agree well with the calculation result.

5. Conclusions

We have examined the feasibility of using spun fibres with an unconventional relationship between their parameters as sensing elements of FOCS's, when the beat length of their built-in linear BR is close to or less than the spin pitch of their helical structure (high σ). It has been shown that the use of fibres with such parameters in the conventional configuration of the sensing element of FOCS's with a $\lambda/4$ plate degrades the interference fringe contrast. The main cause of the decrease in contrast is the increase in the incoherent component of the broadband radiation. To obtain a nearly 100% contrast, we proposed a modified sensing element configuration in which a specially designed phase plate is used instead of the $\lambda/4$ plate and a second phase plate is placed at the output end of the sensing fibre loop.

For experimental verification, we produced sensing elements of FOCS's based on high-σ spun fibre ($\sigma = 0.62$) in the conventional and modified configurations. The interference fringe contrast in the modified configuration (89.4%) was twice that in the conventional configuration.

We investigated the magneto-optical sensitivity of spun fibres differing in σ in a wide spectral region. Reducing the beat length of the built-in linear BR of the spun fibre at a constant spin pitch of its helical structure (increasing its σ) slightly reduces the magneto-optical sensitivity of the spun fibre, which is the result of the decrease in the average ellipticity of the PS of broadband radiation in the spun fibre and is independent of the configuration used.

In conclusion, note again that the proposed modified sensing element considerably improves the threshold sensitivity (detectivity) of FOCS's when high-σ spun fibres are used, in particular in the case of high built-in BR fibres, where the spin pitch exceeds the beat length. Fibres with such parameters are needed e.g. in the fabrication of small sensing elements capable of operating in limited space, as well as in designing vibration-resistant current sensors in which fibre stable to external influences should be used. At the same time, the slight reduction in magneto-optical sensitivity in such fibres is independent of the sensing element configuration and can be compensated for by increasing the number of turns in the coil.

References

1. Frosio G., Dancliker R. *Appl. Opt*., **33**, 6111 (1994).
2. Przhiyalkovsky Ya.V., Morshnev S.K., Starostin N.I., Gubin V.P. *Kvantovaya Elektron*., **43** (2), 167 (2013) [*Quantum Electron*., **43** (2), 167 (2013)].
3. Chamorovsky Yu.K., Starostin N.I., Ryabko M.V., et al. *Opt. Commun*, **282**, 4618 (2009).
4. Gubin V.P., Isaev V.A., Morshnev S.K., et al. *Kvantovaya Elektron*., **36** (3), 287 (2006) [*Quantum Electron*., **36** (3), 287 (2006)].
5. Michie A., Canning J., Bassett I., et al. *Opt. Express*, **15**, 1811 (2007).
6. Gubin V.P., Morshnev S.K., Starostin N.I., et al. *Kvantovaya Elektron*., **41** (9), 815 (2011) [*Quantum Electron*., **41** (9), 815 (2011)].
7. McIntyre P., Snyder A.W. *J. Opt. Soc. Am*., **68** (2), 149 (1978).
8. Hung-chia Huang. *Appl. Opt*., **36** (18), 4241 (1997).

9. Rose A.H., Etzel S.M., Wang C.M. *J. Lightwave Technol*., **15**, 803 (1997).
10. Morshnev S.K., Gubin V.P., Przhiyalkovsky Ya.V., Starostin N.I. *Kvantovaya Elektron*., **43** (12), 1143 (2013) [*Quantum Electron*., **43** (12), 1143 (2013)].
11. Gubin V.P., Morshnev S.K., Starostin N.I., et al. *Radiotekh. Elektron*., **53**, 971 (2008).